Liquid Crystals Embedded in Polymeric Electrolytes for Quasi-Solid State Dye-Sensitized Solar Cell Applications

Sung Chul Kim, Myungkwan Song, Tae In Ryu, Myung Jin Lee, Sung-Ho Jin,* Yeong-Soon Gal, Hyeon-Kyung Kim, Gi-Dong Lee,* Yong Soo Kang

A new series of liquid crystal embedded in polymeric electrolytes was developed for obtaining high efficiency in quasi-solid state dye-sensitized solar cells (DSSCs). The polymeric electrolytes were composed of iodide and tri-iodide redox species in polyacrylonitrile (PAN) as a polymer matrix and liquid crystals (E7 or ML-0249) for increasing the order parameter of electrolyte components with easy transport of redox species. The highest efficiency (6.21 and 6.29% at 1 sun) was obtained for the quasi-solid state DSSCs using E7 to PAN and ML-0249 to PAN, respectively, under AM 1.5 G illumination and an aperture mask condition. The high efficiencies of the quasi-solid state DSSCs are due to the effective formation of pathways through liquid crystal orientation for the transport of redox species.

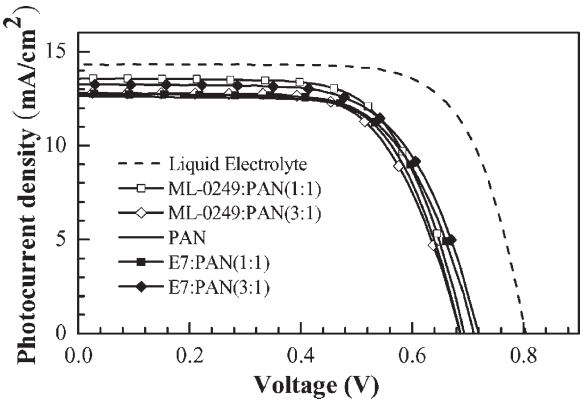

Introduction

In recent days, the conversion of solar to electrical energy has become important due to the crisis in conventional energy sources. There are various natural resources available to generate energy. Converting solar energy into electrical energy is one such exploitation of natural sources. Silicon-based inorganic solar cells are the best utilized for the last few decades in this direction. However, drawbacks such as manufacturing costs and a cumbersome fabrication process made researchers look into easily processable, low cost materials. Since the report from the Grätzel group,[1] dye-sensitized solar cells (DSSCs) have received much attention from researchers. The Grätzel group reported a power conversion efficiency (PCE) of 11% using a liquid electrolyte and its efficiency was very close to the amorphous silicon-based inorganic solar cells.[2] Although DSSCs based on liquid electrolytes have reached as high as 11% under AM 1.5 G 1 sun light intensity (100 mW · cm^{-2}), it has a demerit in that the liquid electrolytes are lost due to leakage and/or volatility of the electrolyte solution, a major drawback that limits DSSC stability. Several significant

S. C. Kim, M. Song, T. I. Ryu, M. J. Lee, S.-H. Jin
Department of Chemistry Education and Interdisciplinary Program of Advanced Information and Display Materials, Pusan National University, Busan 609-735, Korea
Fax: +82-51-581-2348; E-mail: shjin@pusan.ac.kr
Y.-S. Gal
Polymer Chemistry Lab, Kyungil University, Hayang 712-701, Korea
H.-K. Kim, G.-D. Lee
Department of Electrical Engineering, Dong-A University, Busan 604-714, Korea
E-mail: gdlee@donga.ac.kr
Y. S. Kang
Department of Chemical Engineering, Hanyang University, Seoul 133-791, Korea

Macromol. Chem. Phys. **2009**, *210*, 1844–1850

DOI: 10.1002/macp.200900289

research works has been carried out to minimize this problem. These approaches include employing a polymeric electrolyte, solid state or quasi-solid state hole conductors and ionic liquid electrolytes for replacing the liquid electrolytes.[3–6] However, the efficiency of these solid state or quasi-solid state DSSCs was unsatisfactory compared to that using the liquid electrolytes due to the low charge transport ability of the *p*-type semiconductors and poor contact of the solid state charge transport materials with the dye coated TiO_2 surface.[7,8] In particular, research on the chemical structure, morphology, optical and electrical properties of the electrolytes plays a significant role in the design of high efficiency DSSCs.

Liquid crystals have been used by many research groups to template inorganic and organic materials, especially polyacetylene and polythiophene derivatives, which increase the carrier mobility and electrical conductivity.[9–11] Room temperature liquid crystals are attractive candidates for replacement of the volatile liquid electrolytes due to the formation of mesophase and high ionic conductivity. Attempts to apply liquid crystals in the field of the organic photovoltaic cells was first reported by the Friend group.[12] The maximum PCE of an organic photovoltaic cell using self-organized discotic liquid crystals was 1.95% at 490 nm. Herein, we report the development of a polymeric electrolyte using liquid crystals and photovoltaic performance of quasi-solid state DSSCs. To the best of our knowledge, this is the first report on the investigation of liquid crystals for the polymeric electrolyte components in DSSCs.

Experimental Part

Fabrication of Dye-Sensitized Solar Cells

DSSCs were fabricated as follows. Screen-printable nc-TiO_2 pastes were prepared using ethyl cellulose (Aldrich), lauric acid (Fluka) and terpineol (Fluka) as described elsewhere.[13] The prepared nc-TiO_2 paste was coated on a FTO conducting glass (TEC8, Pilkington, 8 Ω cm^{-1}, glass thickness of 2.3 mm), dried in air at ambient temperature for 5 min and sintered at 500 °C for 30 min. The thicknesses of the annealed films were measured with an Alpha-step IQ surface profiler (KLA Tencor). For dye adsorption, the annealed nc-TiO_2 electrodes were immersed in absolute ethanol containing 0.5×10^{-3} M N719 dye ($Ru[LL'(NCS)_2]$, L = 2,2′-bypyridyl-4,4′-dicarboxylic acid, L′ = 2,2′-bypyridyl-4,4′-ditetrabutylammonium carboxylate) for 24 h at ambient temperature. N719 dye was chromatographically purified. Pt counter electrodes were prepared by thermal reduction of a thin film formed from 7×10^{-3} M H_2PtCl_6 in 2-propanol at 400 °C for 20 min. The dye-adsorbed nc-TiO_2 electrode and Pt counter electrode were assembled using 60 μm-thick Surlyn® (Dupont 1702). The liquid crystal embedded in polymeric electrolyte was composed of iodine (I_2), tetrabutylammonium iodide (TBAI), 1-propyl-3-methylimidazolium iodide (PMII) as an ionic liquid, ethylene carbonate (EC)/propylene carbonate (PC) (3/1 as weight ratio), polyacrylonitrile (PAN) ($\overline{M}_w = 86\,200$, Aldrich Co) as a polymeric matrix, a liquid crystal (Merck Co) as a plasticizer, and acetonitrile (AN). The liquid crystal embedded in polymeric electrolytes was filled between two electrodes using a vacuum pump on a hotplate. A uniform liquid crystal embedded in the polymeric electrolyte layer was formed in the cells after cooling down to room temperature. The active areas of the dye-coated TiO_2 films were measured by an image analysis program equipped with a digital microscope camera (Moticam 1000).

Photovoltaic Measurements

The conductivity measurements were carried out with the polymer coated onto the pre-patterned ITO cell. The thickness of the polymer layer was about 100 μm. The a.c. complex impedance was recorded using an impedance analyzer (Zahner Elektrik, model IM6) in the frequency range 1 Hz to 1 MHz. The temperature of the sample was controlled by means of a programmable hot plate (Mettler, model FP82HT). All samples were prepared in an argon gas filled glove box. Photocurrent-voltage measurements were performed using a Keithly model 2400 source unit. A class-A solar simulator (Yamashita Denso, model YSS-200A) equipped with a 1 600 W Xenon lamp as a light source, where light intensity was adjusted using a Fraunhofer ISE-calibrated mono Si solar cell with KG-3 filter for approximating AM 1.5 G 1 sun light intensity. During photocurrent-voltage measurement, the DSSC was covered with a black mask with an aperture to avoid additional light coming through lateral space.[14,15] Incident photon to current conversion efficiency (IPCE) was measured as a function of wavelength from 300 to 800 nm using a specially designed IPCE system for DSSCs (PV measurements, Inc.). A 75 W Xenon lamp was used as a light source for generating a monochromatic beam. Calibration was performed using a silicon photodiode, which was calibrated using a NIST-calibrated photodiode G425 as a standard, and IPCE values were collected under bias light at a chopping speed of 10 Hz. The electrochemical impedance spectra were measured with a potentiostat (Solartron 1287) equipped with a frequency response analyzer (Solartron 1260), with the frequency ranging from 10^{-1} to 10^6 Hz. The magnitude of the alternative signal was 10 mV. Impedance parameters were determined by fitting of impedance spectrum using Z-view software. The impedance measurements were carried out at open-circuit potential under AM 1.5 G 1 sun light illumination.

Results and Discussion

We used liquid crystals as a component of polymeric electrolytes for the fabrication of quasi-solid state DSSCs in order to improve the photovoltaic performance. The liquid crystal was selected as E7 having CN– as the terminal group, due to the fact that PAN as a polymer matrix for liquid crystal embedded in polymeric electrolyte induced molecular similarity between the E7 and PAN. The E7 was made of four CN-biphenyls at a given composition, as

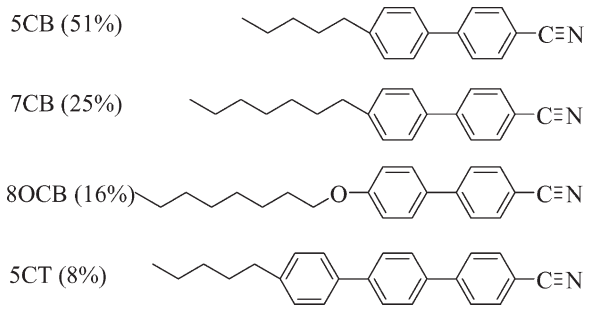

Figure 1. Molecular structures and composition of E7 liquid crystal.

shown in Figure 1, which is widely used in polymer dispersed liquid crystalline (PDLC) displays.[16] Another liquid crystal mixture used in this experiment was ML-0249, which possesses a good combination of high dielectric anisotropy ($\Delta\varepsilon = 8.4$) and low rotational viscosity ($g_1 = 73$ mPass). ML-0249 can be currently used for TFT-LCDs with the advantage of fast response time and low driving voltage. The direct addition of liquid electrolytes onto PAN and liquid crystals (E7 or ML-0249) without in situ polymerization was found to be an important approach for the fabrication of quasi-solid state DSSCs. The liquid crystal embedded in polymeric electrolytes were prepared by blending a mixture of PAN, EC, PC, AN, TBAI, I_2, PMII, and a desired concentration of liquid crystals at room temperature for 24 h. As reported ever since, the current article focused on the introduction of liquid crystals into polymeric electrolyte in the field of quasi-solid state DSSCs and investigated the photovoltaic performance. High photovoltaic performance was achieved by increasing the molecular order and ionic conductivity of the liquid crystal embedded in polymeric electrolytes with the formation of redox species through the transport of diffusion pathways, as reported earlier.

Figure 2 shows the hypothesized orientation of liquid crystal embedded in polymeric electrolytes for quasi-solid state DSSCs. In general, the diffusion rate of the redox species between electrolyte molecules, which determines the transfer probability of the redox species, is mainly dependent on the distance between the molecules and the ordering strength of the electrolyte molecules. Therefore, the high order parameter of the liquid crystal embedded in polymeric electrolyte molecules induced the transport pathway for high transfer probability of redox species which led to an increase in photocurrent density and improved photovoltaic performance. In Figure 2, the liquid crystal directors in the liquid crystal embedded in polymeric electrolytes look arbitrarily aligned in each direction in the macroscopic view. However, in the molecular dimension, the liquid crystal molecules neighboring will be aligned in almost the same direction to each other

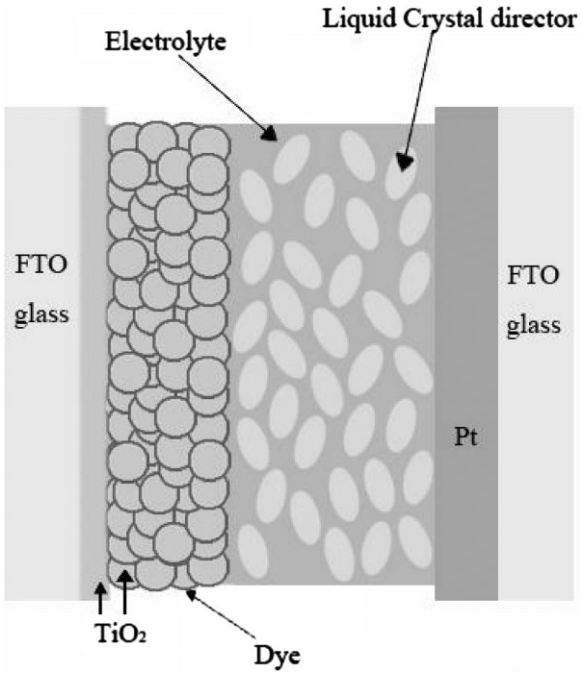

Figure 2. The cross-section structure of the quasi-solid state DSSC using liquid crystal embedded in polymeric electrolyte.

because the liquid crystal director can handle as a continuum. Thus, it induced the increased ordering strength of the liquid crystal embedded in polymeric electrolytes and enhanced the transport of redox species through the liquid crystal induced diffusion pathway in the quasi-solid state DSSCs. Generally, the scalar order parameter of the liquid crystals was measured in the range 0.5–0.7 at room temperature.

In order to prove the role of the liquid crystals, we measured the electro-optical response of the quasi-solid state DSSCs, to prove the ordered state of the quasi-solid state DSSCs, not the isotropic state. We observed spatially partial optical switching in the quasi-solid state DSSCs due to the small concentration of the liquid crystals and solidification in the quasi-solid state DSSCs. Figure 3 shows the measured optical response of the quasi-solid state DSSCs with an applied voltage of ± 8 V at a frequency of 16 Hz under cross-Nicol polarizers. The liquid crystal molecules were ML-0249. In Figure 3, t_1 and t_3 represent the time position to apply the a.c. voltage and t_2 and t_4 represent the time position to cut the applied voltage off. We observed the rapid optical peak at t_1 and t_3, and it is shown in Figure 3. This occurs by fast moving up of the liquid crystal directors by the high applied voltage. On the contrary, at t_2 and t_4, which is the voltage cut off state, the ML-0249 in the quasi-solid state DSSCs moves down again because the external voltage is cut off. From Figure 3, it can be observed that it had a lower decay time than its

Macromol. Chem. Phys. **2009**, *210*, 1844–1850

Macromolecular Journals

DOI: 10.1002/macp.200900289

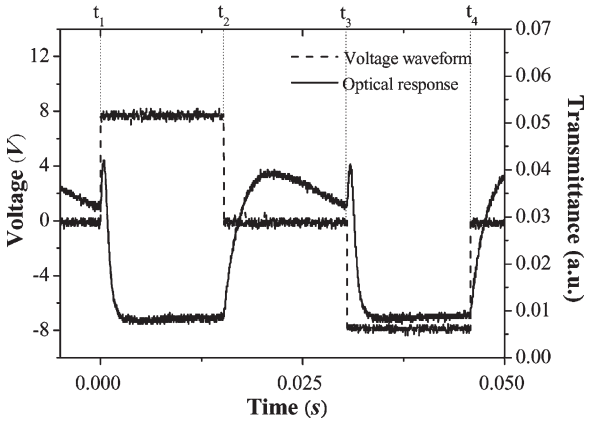

Figure 3. Measured electro-optical response of the quasi-solid state DSSCs with liquid crystal embedded in polymeric electrolyte between cross-Nicol polarizers.

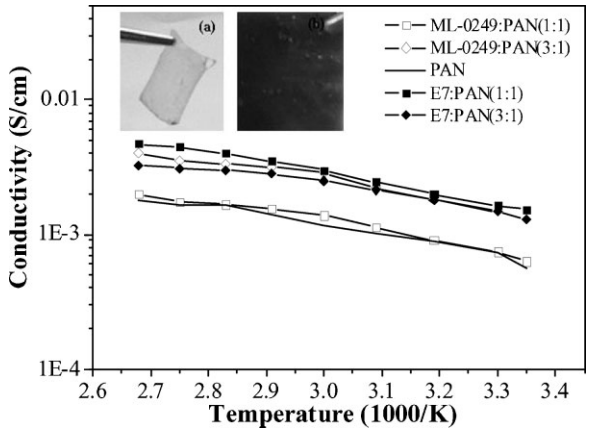

Figure 4. Temperature dependence of ionic conductivity on liquid crystal embedded in polymeric electrolytes and PAN-based electrolyte. Inset: Photographs of liquid crystal embedded in polymeric electrolyte films with E7 (a) and ML-0249 (b).

corresponding rising time since the decay time of the liquid crystal directors depends on the viscosity of the surrounding material and their elastic constant. The high viscosity of the liquid crystal embedded in polymeric electrolytes may prevent a fast switching response. From these results, it was confirmed that the liquid crystal molecules play a significant role in increasing the order parameter of the liquid crystal embedded in polymeric electrolytes for better photocurrent density.

In general, the PCE of DSSCs is mainly dependent on the ionic conductivity of the polymeric matrix. It has been found that the ionic conductivity of the polymeric electrolytes can be increased by incorporating suitable plasticizers or additives.[17,18] Typically, the ionic conductivity of PAN:$LiCF_3SO_3$ and PEG:$LiBF_4$ complex was about 10^{-3} and 10^{-6}–10^{-7} $S \cdot cm^{-1}$, respectively.[19,20] Figure 4 shows a comparison of the ionic conductivity of the liquid crystal embedded in polymeric electrolytes between the different content of liquid crystals and PAN. Among the different ratio of liquid crystals, the ionic conductivity of E7:PAN (1:1) complex was 2.2×10^{-3} $S \cdot cm^{-1}$ at room temperature, which was 2.5 times higher than that of PAN-based electrolyte at room temperature. Both short-circuit photocurrent density (J_{sc}) and fill factor (*FF*) were influenced by the ionic conductivity of the polymeric electrolyte, because low conductivity causes low charge transport and increases the series resistance. The higher ionic conductivity of liquid crystal embedded in polymeric electrolytes was due to the introduction of liquid crystals, which induced ease of transport for redox species with the increase in ionic movement in liquid crystal embedded in polymeric electrolytes. After casting the liquid crystal embedded in polymeric electrolyte on a glass substrate using a doctor blade on a hotplate, the solvent was evaporated to obtain a film as shown in the inset of Figure 4. The thickness of the quasi-solid state DSSCs was about 10 μm of a TiO_2 deposited layer and 3 μm of a liquid crystal embedded in polymeric electrolyte layer measured by scanning electron microscopy (SEM) and Alpha-step IQ, respectively.

In order to investigate the optimum weight ratio of liquid crystals and PAN, the photovoltaic performances of quasi-solid state DSSCs were compared with different weight ratios of liquid crystals and PAN as plasticizer and polymer matrix, respectively. The photovoltaic characteristics of the quasi-solid state DSSCs fabricated with 3:1, 1:1, and 0:1 ratio of liquid crystals and PAN are presented in Figure 5 and the parameters are summarized in Table 1.

Figure 5 compares the photocurrent density-voltage (*J-V*) curves and the IPCE spectra of quasi-solid state DSSCs with liquid crystal embedded in polymeric electrolytes and PAN-based electrolyte and liquid electrolyte for comparison. All quasi-solid state DSSCs were obtained by a similar device assembly and measurement procedures. Encouraging results showed that the liquid crystal embedded in polymeric electrolytes improved the photovoltaic performance in comparison with PAN-based electrolyte, except for ML-0249:PAN (3:1) at 1 sun intensity. Among the several combinations used, ML-0249:PAN (1:1) device showed a V_{oc} of 0.703 V, J_{sc} of 13.57 $mA \cdot cm^{-2}$, fill factor of 0.668, and PCE of 6.29% at 1 sun intensity, and increased to 6.48% at 0.43 sun intensity. In the case of E7 and PAN-based liquid crystal embedded in polymeric electrolytes, the optimum blending ratio was 3:1 and the E7:PAN (3:1) device exhibited a V_{oc} of 0.719 V, J_{sc} of 13.27 $mA \cdot cm^{-2}$, fill factor of 0.651 and PCE of 6.21% at 1 sun intensity and this was found to increase to 6.94% at 0.43 sun intensity. The fill factor (*FF*) was influenced by the contact resistance between the TiO_2 surface and electrolyte. Generally, the polymeric electrolytes had less contact and compatibility with the TiO_2

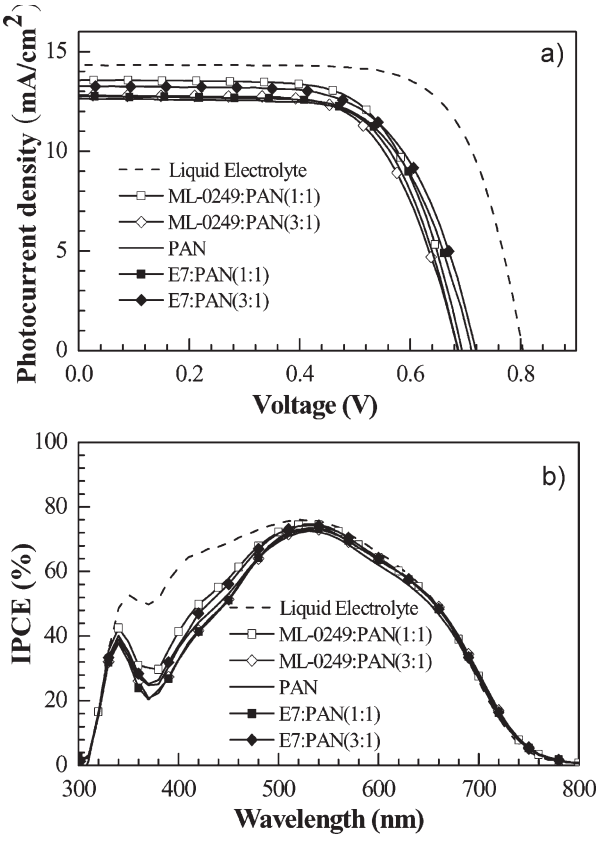

Figure 5. (a) *J-V* curves under AM 1.5 G 1 sun illumination (100 mW · cm^{-2}) and (b) IPCE spectra of quasi-solid state DSSCs with liquid crystal embedded in polymeric electrolytes along with PAN-based electrolyte and liquid electrolyte. Each DSSC for *J-V* measurement was covered with an aperture mask to eliminate additional light.

Table 1. The photovoltaic performances of quasi-solid state DSSCs with liquid crystal embedded in polymeric electrolyte and liquid electrolyte for comparison. Each cell was covered with an aperture mask during measurement. Reduction of light intensity was performed with a mesh grid. Composition of liquid crystal embedded in polymeric electrolyte: 200 mg of 1-propyl-3-methy imidazolium iodide (PMII), 180 mg of tetrabutylammonum iodide (TBAI), 60 mg of I_2, 600 mg of ethylene carbonate (EC), 200 mg of propylene carbonate (PC), and 400 mg as the total weight of ML-0249 and PAN in 0.2 ml of acetonitrile solution. Liquid electrolyte was composed of 0.7 M PMII, 0.03 M I_2, 0.05 M guanidinium thiocyanate (GuSCN), 0.5 M 4-*tert*-butylpyridine (TBP) in acetonitrile and valeronitrile (v/v 85:15).

1 sun (100 mW · cm^{-2})	J_{SC}	V_{OC}	*FF*	Eff	area
	MA · cm^{-2}	**V**	**%**	**%**	**cm^2**
ML-0249:PAN(1:1)	13.57	0.703	66.8	6.29	0.288
ML-0249:PAN(3:1)	12.81	0.686	66.3	5.83	0.263
PAN	12.64	0.687	68.5	5.95	0.244
E7:PAN(1:1)	12.75	0.711	66.4	6.01	0.289
E7:PAN(3:1)	13.27	0.719	65.1	6.21	0.255
Liquid Electrolyte	14.32	0.804	71.5	8.24	0.261
0.43 sun (43 mW · cm^{-2})	J_{SC}	V_{OC}	FF	Eff	area
	MA · cm^{-2}	**V**	**%**	**%**	**cm^2**
ML-0249:PAN(1:1)	6.31	0.644	68.6	6.48	0.288
ML-0249:PAN(3:1)	6.06	0.637	69.3	6.22	0.263
PAN	5.76	0.631	71.1	6.01	0.244
E7:PAN(1:1)	6.09	0.671	69.1	6.57	0.289
E7:PAN(3:1)	6.31	0.691	68.4	6.94	0.255
Liquid Electrolyte	6.31	0.786	73.3	8.45	0.261
0.11 sun (11 mW · cm^{-2})	J_{SC}	V_{OC}	*FF*	Eff	area
	mA · cm^{-2}	**V**	**%**	**%**	**cm^2**
ML-0249:PAN(1:1)	1.70	0.569	72.7	6.39	0.288
ML-0249:PAN(3:1)	1.62	0.567	72.7	6.07	0.263
PAN	1.55	0.564	74.3	5.90	0.244
E7:PAN(1:1)	1.60	0.603	73.1	6.41	0.289
E7:PAN(3:1)	1.63	0.629	71.2	6.64	0.255
Liquid Electrolyte	1.69	0.729	73.1	8.19	0.261

surface compared to liquid electrolyte, which increased the surface resistance and series resistance. From these results, *FF* values of PAN with liquid crystal decreased in comparison with the case of the liquid electrolyte in Table 1.

As shown in Table 1, a minor deviation in PCE was observed for the liquid crystal embedded in polymeric electrolytes even then the intensity of light was reduced from 1 sun to 0.11 sun, which highlights that transport of redox species was independent of light intensity in the liquid crystal embedded in polymeric electrolytes. As far as investigated, it was the highest PCE obtained that has been ever reported for quasi-solid state DSSCs with polymeric electrolytes.[21–25] The photocurrent action spectrum is shown in Figure 5(b). The incident photon-to-current conversion efficiency (IPCE) of liquid crystal embedded in polymeric electrolytes and liquid electrolyte reached a maximum efficiency of 80% at 540 nm.

Figure 6 shows the dependence of photocurrent density on light intensity. Except for the slight deviation at around 1 sun light intensity compared with liquid electrolyte cell, photocurrent densities for liquid crystal embedded in polymeric electrolytes are linearly proportional to light intensity. This linearity implied that photocurrent was neither limited by the diffusion of iodide and tri-iodide redox species nor by their migration. The reasonably good conductivity of the liquid crystal embedded in polymeric electrolytes for the redox species rationalizes the linearity.

Macromol. Chem. Phys. **2009**, *210*, 1844–1850

Macromolecular Journals

DOI: 10.1002/macp.200900289

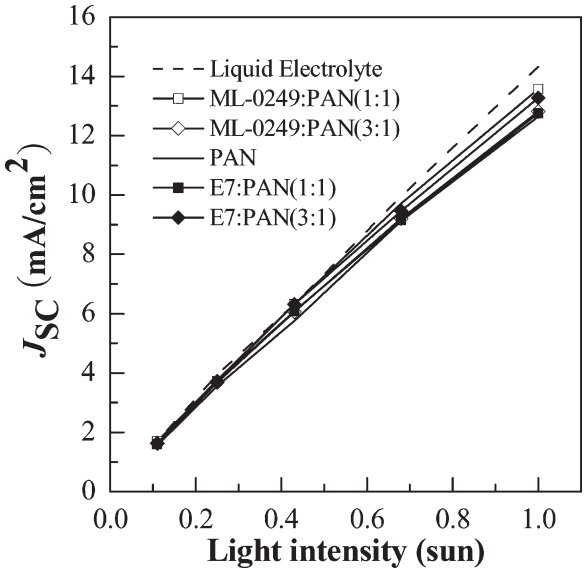

Figure 6. Dependence of photocurrent density on light intensity for quasi-solid state DSSCs with liquid crystal embedded in polymeric electrolytes along with PAN-based electrolyte and liquid electrolyte.

It suggests that the liquid crystal with its flexibility can retain polymer electrolytes in its pores, and the liquid crystal embedded in polymeric electrolytes can percolate freely, thereby giving good ionic conductivity. It was assumed that the liquid crystal embedded in polymeric electrolytes had close contact and compatibility with the TiO_2 surface which allowed free space for the movement of redox species. It was reflected by the high J_{sc}, V_{oc}, and linearity between J_{sc} and illumination intensity obtained as above. Thus it indicates that there was almost no mass transport problem in the liquid crystal embedded in polymeric electrolytes. As a result, PCE is almost the same regardless of light intensity, as can be seen in Table 1.

Figure 7 and Table 2 compare the electrochemical impedances of liquid crystal embedded in polymeric electrolytes with PAN-based electrolyte and liquid electrolyte for comparison. The Cole-cole plots in Figure 7 can be fitted with an equivalent circuit with Rs, R1, R2 and R3, where Rs, R1, R2 and R3 represent FTO sheet resistance, charge transfer resistance at Pt/electrolyte (and/or FTO/electrolyte) interface, charge transfer resistance at TiO_2/dye/electrolyte interface and electrolyte solution resistance. Although slightly higher R3 values due to increased viscosity are seen, it was noted that most interfacial charge transfer resistances for liquid crystal embedded in polymeric electrolytes are very close to that for liquid electrolyte, which suggests that the liquid crystal embedded in polymeric electrolytes shows liquid-like behavior.

Table 2. Resistances in equivalent circuit for quasi-solid state DSSCs with liquid crystal embedded in polymeric electrolyte and liquid electrolyte.

	R_S[a)]	$R1$[a)]	$R2$[a)]	$R3$[a)]
	Ω	Ω	Ω	Ω
ML-0249:PAN(1:1)	4.99	2.63	11.0	6.98
ML-0249:PAN(3:1)	5.50	3.70	12.8	9.95
PAN	4.99	3.89	13.9	8.64
E7:PAN(1:1)	5.43	3.91	10.0	9.59
E7:PAN(3:1)	5.29	5.52	11.1	9.72
Liquid Electrolyte	5.01	3.46	11.9	3.56

[a)] *Rs*, *R*1, *R*2 and *R*3 represent FTO sheet resistance, charge transfer resistance at Pt/electrolyte (and/or FTO/electrolyte) interface, charge transfer resistance at TiO_2/dye/electrolyte interface and electrolyte solution resistance.

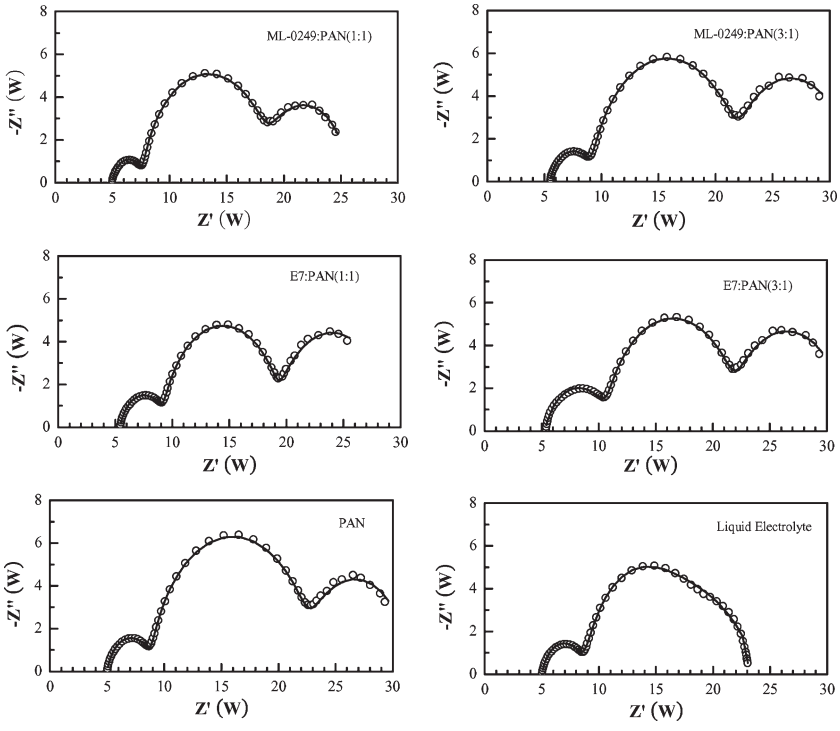

Figure 7. Electrical impedance spectra for quasi-solid-state DSSCs with liquid crystal embedded in polymeric electrolytes along with PAN-based electrolyte and liquid electrolyte. Measurements were performed at open-circuit potential under 1 sun illumination.

Conclusion

In summary, a new series of liquid crystal embedded in polymeric electrolytes were developed for obtaining high efficiency quasi-solid state dye-sensitized solar cells (DSSCs). After casting the electrolyte onto a dye coated TiO_2 surface, the electrolyte was quasi-solid state in nature, but performed similarly to liquid electrolyte. The higher ionic conductivity of the liquid crystal embedded in polymeric electrolytes leads to enhancement in both J_{sc} and fill factor of the quasi-solid state DSSCs, which significantly improved the photovoltaic performance. The overall PCE of the newly developed liquid crystal embedded in polymeric electrolyte was 6.29% (at a 1:1 weight ratio of ML-0249:PAN). The quasi-solid state DSSCs showed comparable PCE to the liquid electrolyte-based DSSC. The verification of the role of liquid crystals in the liquid crystal embedded in polymeric electrolytes was performed with measurement of the electro-optical response of quasi-solid state DSSCs under cross-Nicol polarizers. The high efficiencies of the quasi-solid state DSSCs are due to the effective formation of a pathway through the liquid crystal orientation for the transport of redox species. Therefore, these results indicate that the problem of low charge transport ability and poor contact with dye coated TiO_2 surface was significantly reduced for enhanced performance of quasi-solid state DSSCs.

Acknowledgements: This work was supported by the *Korea Science and Engineering Foundation (KOSEF)* grant funded by the *Korea government (MOST)* (No. M10600000157-06J0000-15710, R11-2008-088-01-003-0).

Received: June 14, 2009; Revised: July 13, 2009; Published online: September 1, 2009; DOI: 10.1002/macp.200900289

Keywords: charge transport; conducting polymers; dyes/pigments; liquid-crystalline polymers (LCP); photochemistry

[1] B. O'Regan, M. Grätzel, *Nature* **1991**, *353*, 737.
[2] M. Grätzel, *J. Photochem. Photobiol. A.* **2004**, *164*, 3.
[3] T. Asano, T. Kubo, Y. Nishikitani, *J. Photochem. Photobiol. A.* **2004**, *164*, 111.
[4] A. F. Nogueira, J. R. Durrant, M. A. De Paoli, *Adv. Mater.* **2001**, *13*, 826.
[5] T. Stergiopoulos, I. M. Arabatzis, G. Katsaros, P. Falaras, *Nano Lett.* **2002**, *2*, 1259.
[6] O. A. Ileperuma, M. A. K. L. Dissanayake, S. Somasundaram, *Electrochim. Acta.* **2002**, *47*, 2801.
[7] H. Kusama, H. Arakawa, *J. Photochem. Photobiol. A.* **2004**, *164*, 103.
[8] P. Wang, S. M. Zakeeruddin, I. Exnar, M. Grätzel, *Chem. Commun.* **2002**, *24*, 2972.
[9] J. Hulvat, J. S. I. Stupp, *Angew. Chem. Int. Ed.* **2003**, *42*, 778.
[10] S. W. Kang, S. H. Jin, L. C. Chien, S. Sprunt, *Adv. Funct. Mater.* **2004**, *14*, 329.
[11] A. Akagi, G. Piao, S. Kaneko, K. Sakamaki, H. Shirakawa, M. Kyotani, *Science* **1998**, *282*, 1683.
[12] M. L. Schmidt, A. Fechtenkötter, K. Müllen, E. Moons, R. H. Friend, J. D. MacKenzie, *Science* **2001**, *293*, 1119.
[13] H. J. Koo, J. Park, B. Yoo, K. Yoo, K. Kim, N. G. Park, *Inorg. Chim. Acta* **2008**, *361*, 677.
[14] S. Ito, M. K. Nazeeruddin, P. Liska, P. Comte, R. Charvet, P. Péchy, M. Jirousek, A. Kay, S. M. Zakeeruddin, M. Grätzel, *Prog. Photovolt: Res. Appl.* **2006**, *14*, 589.
[15] J. Park, H. J. Koo, B. Yoo, K. Yoo, K. Kim, W. Choi, N. G. Park, *Solar Energy Mater. Solar Cells* **2007**, *91*, 1749.
[16] D. W. Rafferty, J. L. Koenig, G. Magyar, J. West, *J. Appl. Spectrosc.* **2002**, *56*, 284.
[17] F. Cao, G. Oskam, P. Searson, *J. Phys. Chem.* **1995**, *99*, 17071.
[18] K. Tennaknoe, G. K. R. Senadeera, V. P. S. Perera, I. R. M. Kottegoda, L. A. De Silva, *Chem. Mater.* **1999**, *11*, 2474.
[19] H. K. Yoon, W. S. Chung, N. J. Cho, *Electrochim. Acta* **2004**, *50*, 289.
[20] B. Kumar, L. G. Scanlon, *Solid State Ionics* **1999**, *124*, 239.
[21] B. Li, L. Wang, B. Kang, P. Wang, Y. Qiu, *Solar Energy Mater. Solar Cells* **2006**, *90*, 549.
[22] P. Wang, S. M. Zakeeruddin, J. E. Moser, M. K. Nazeeruddin, T. Sekiguchi, M. Grätzel, *Nature Materials* **2003**, *21*, 402.
[23] J. Wu, Z. Lan, J. Lin, M. Huang, S. Hao, T. Sato, S. Yin, *Adv. Mater.* **2007**, *19*, 4006.
[24] P. Wang, S. M. Zakeeruddin, M. Grätzel, *J. Fluorine Chemistry* **2004**, *125*, 1241.
[25] T. Kato, A. Okazaki, S. Hayase, *Chem. Commun.* **2005**, 363.

DOI: 10.1002/macp.200900289